11TH JOINT MMM–INTERMAG CONFERENCE

January 18–22, 2010
Washington, DC

DIGESTS

HELP CONTINUE

CONFERENCE INFORMATION

www.magnetism.org

Published by the American Institute of Physics (AIP).

 ISSN 1087-3848

Novel Double-barrier Rotor Designs in Interior-PM Motor For Reducing Torque Pulsation

Liang Fang, Sung-Il Kim, Jung-Pyo Hong, *Senior, IEEE*

Department of Automotive Engineering, Hanyang University, Seoul 133-791, Korea

This paper presents various flux-barrier designs in an interior permanent magnet synchronous motor (IPMSM) for reducing the torque pulsation. A conventional single-layer IPMSM model, a popular double-layer IPMSM model and two proposed novel double-barrier IPMSM models, feature as the simplest single-layer PM coupled with flexible double pairs of flux-barrier, are built and optimized for minimizing cogging torque and torque ripple. The optimal geometries of flux-barrier structure in each IPMSM designs are determined by performing response surface methodology (RSM). The cogging torque and torque ripple of IPMSM are calculated by using finite element analysis (FEA), and confirmed by test. Finally, the validity and advantages of the novel double-barrier IPM rotor designs on torque performance improvement are emphasized.

***Index Terms*—FEA, IPMSM, novel double-barrier designs, RSM, torque pulsation reduction.**

I. Introduction

THE INTERIOR permanent magnet synchronous motors (IPMSM) are widely used in home application, industrial, and electric and hybrid vehicle (HEV) propulsion, due to their high efficiency, high torque density and wide speed range [1].

However, the IPM machines usually have significant torque pulsation problem, result in vibration, noise, and damage to drive components [2]. The removal of torque pulsation is an essential requirement for high-performance application [3].

Torque ripple of output average torque is caused by the interaction of the rotor field and stator currents, which related to the harmonic in the Back-EMF. And, cogging torque arises from the interaction between the air-gap flux distribution and slotted stator structure, is another key components of torque pulsation. Thereby, the torque performance can be improved by reducing the torque ripple of average torque, as well as minimizing the cogging torque production [3].

One of the well known approaches to minimize torque ripple and cogging torque of IPMSM is rotor inner flux path design, such as by drilling small circular holes in the rotor appear in [4]. In this paper, the shapes of flux-barrier structure in IPM rotor are optimized for effectively distributing the magnet flux crossing into the air-gap with desired waveform.

The single-layer IPMSM is the most conventional, as Fig.1 shows, that only one pair of flux-barrier coupled with each PM. In recent years, the double-layer IPMSM designs are popularly adopted since their more flexible flux-barrier design help to improve the torque performance further [5]. In simple case, the double-layer IPMSM can be built by splitting the single-layer IPM segment into two layers, which also creating double pairs of flux-barrier used for changing the flux path inside the rotor. It should be noticed that the double-layer IPM design will unavoidably increase the manufacture cost and difficulty, and even may cause severe irreversible demagnetization [5].

Therefore, this paper proposes two novel double-barrier IPM rotor designs, featuring as each buried single-layer PM segment creates double pairs of flux-barrier. That is, the novel IPM rotor designs have beneficial attribute of the flexible flux-barrier of double-layer IPMSM in design, and the simplicity of single-layer IPMSM in manufacture.

Manuscript received October 31, 2009. Corresponding author: Jung-Pyo Hong (e-mail: hongjp@hanyang.ac.kr)

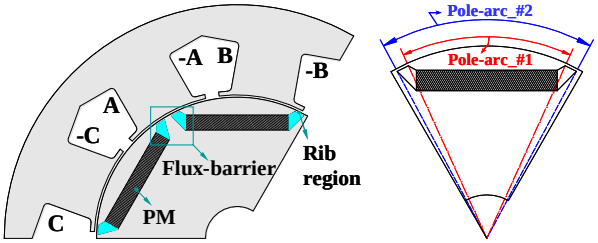

Fig. 1. Configuration of conventional single-layer IPMSM model.

With the help of response surface methodology (RSM), the shapes of buried flux-barrier structure in each mentioned IPMSM models are optimized for reducing torque ripple and cogging torque. Finite element analysis (FEA) and test method are used for examining the effectivity of proposed novel flux-barrier IPM rotor designs on torque pulsation reduction.

II. Model and Characteristic Analysis

A. Prototype Analysis Model

Fig. 1 shows a prototype 6-pole/9-slot IPMSM model for a driving compressor in HEV. The main dimension and specifications are listed in TABLE I. The stator has 3-phase concentrated windings, and the rotor adopts conventional single-layer IPM design. The magnet pole-arc is precisely determined in term of “pole-arc_#1” and “pole-arc_# 2” with considering rib regions between the barriers and rotor surface.

TABLE I
Dimensions and Specifications of Driving Compressor IPMSM

Items	Value	Unit
Stator/Rotor outer diameter	117.2 / 70.8	mm
Stack length / Air-gap length	15 / 0.6	mm
B_r (@20~25℃)	1.22~1.28	T
Maximum terminal voltage	98.6	V
Rated output power	2	kW
Maximum current	17	A_{rms}
Base speed	3500	rpm

B. Torque Characteristic Analysis

In this paper, the equivalent circuit method is introduced for analyzing the machine performance at steady-state condition, and then the output torque and cogging torque characteristic of IPMSM are preciously calculated by FEA.

In a *d-q* reference frame, a well accepted equivalent circuit with iron loss consideration is given, as Fig. 2 gives [6]. And the corresponding mathematical models of *d-q* axis circuit are obtained, voltages and currents are given as equations (1) and (2), and output torque is expressed as equations (3).

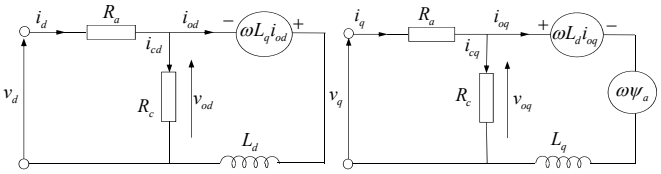

(a) *d*-axis equivalent circuit (b) *q*-axis equivalent circuit

Fig. 2. Equivalent circuits of IPMSM with iron loss consideration

$$\begin{bmatrix} v_d \\ v_q \end{bmatrix} = R_a \begin{bmatrix} i_{od} \\ i_{oq} \end{bmatrix} + \left(1+\frac{R_a}{R_c}\right)\begin{bmatrix} v_{od} \\ v_{oq} \end{bmatrix} + p\begin{bmatrix} L_d & 0 \\ 0 & L_q \end{bmatrix}\begin{bmatrix} i_{od} \\ i_{oq} \end{bmatrix} \quad (1)$$

$$\begin{bmatrix} v_{od} \\ v_{oq} \end{bmatrix} = \begin{bmatrix} 0 & -\omega L_d \\ \omega L_d & 0 \end{bmatrix}\begin{bmatrix} i_{od} \\ i_{oq} \end{bmatrix} + \begin{bmatrix} 0 \\ \omega\psi_a \end{bmatrix} \quad (2)$$

$$\begin{aligned} T &= P_n[\psi_a i_q + (L_d - L_q) i_d i_q] \\ &= P_n[\psi_a I_a \cos\beta + \frac{1}{2}(L_d - L_q) I_a{}^2 \sin 2\beta] \end{aligned} \quad (3)$$

where i_d, i_q: *d-*, *q*-axis components of armature current; v_d, v_q: *d-*, *q*-axis components of terminal voltage; ψ_a: $\sqrt{3/2}\,\psi_f$; ψ_f: maximum flux linkage of permanent magnet; R_a: armature winding resistance; R_c: iron loss equivalent resistance, L_d, L_q: inductance along *d-*, *q*-axis; $p = d/dt$; P_n: number of pole pairs.

By performing the above *d-q* axis equivalent circuits, the IPMSM output performances can be predicted quickly. The entire speed range operation considering the given control conditions are acquired as that: in the anterior region of base speed, maximum torque per ampere control is employed, and flux weakening control is applied in the posterior region. Fig. 3 shows the results of output torque and power performance, as well as the input current I_a and phase angle β. With this the torque characteristic at any speed operation can be calculated by FEA. From the torque equation (3), the output torque is predicted with the magnet flux linkage ψ_a, and input current I_a coupled with phase angle β. Correspondingly, the L_d and L_q must be computed according to the variations of I_a and β.

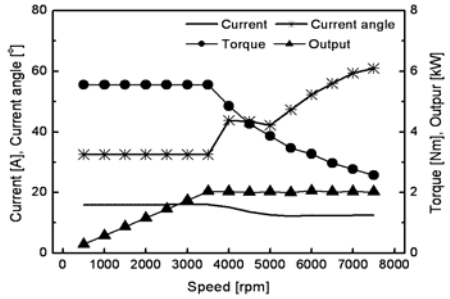

Fig. 3. Speed versus torque and output performance of IPMSM model.

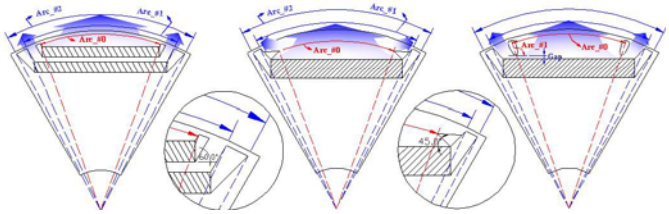

(a) (b) (c)

Fig. 4. Flux distribution in various double pairs flux-barrier rotor designs, (a) double-layer IPMSM design, (b) novel double-barrier design_A: "joint" barriers, (c) novel double-barrier design_B: "separate" barriers.

C. Flexible Flux-barrier Designs

The mentioned various flux-barrier designs in IPMSM on torque pulsation reduction are built and examined. Base on the prototype single-layer IPMSM model, a double-layer IPM rotor model is built by splitting the same PM segment into two layers, which accordingly creates two pairs of separated flux-barriers, as Fig. 4(a) illustrates. In addition, two novel double-barrier IPM rotor model are proposed, featuring as the buried single-layer PM has two pairs of flux-barriers. Novel design A creates "joint" type flux-barrier, as Fig. 4(b) shows and novel design B has a "separate" flux-barrier closed to the rotor surface and magnet surface, as Fig. 4(c) illustrate. Both of the two novel designs can also effectively change the PM flux path distribution in the rotor. The magnet flux crossing into the air-gap with the similar way as the f double-layer IPM design, but the cost and difficult in manufacture is decreased, and the irreversible demagnetization under large input current is avoided. The design variables of all above flux-barrier designs are given in their respective models.

III. Optimization of Flux-barriers in IPMSM

The IPM rotor inner geometry design is very complicated owing to many design factors, and also mechanical robustness between each part must be fully considered in modeling [5]. Therefore, the presented flux-barrier designs in IPM rotor are optimized by introducing response surface methodology (RSM). As an effective approach, RSM is usually applied for searching the optimal design of electrical devices in order to improve machine performances [7]. It is a set of statistical and mathematical techniques to find the "best fitted" response of the physical system through experiment or simulation [8].

For examining the influence of flux-barriers design on torque pulsation reduction, the given design variables, including magnetic "Arc" and "position" , are chosen as design variables in RSM analysis. For decreasing design difficulty, three variables at most are chosen to describe the two pairs of flux-barriers in IPM rotor designs, with the non-significant variable fixed to be proper constant, as Fig. 4 given.

TABLE II
RANGES OF DESIGN VARIABLES FOR OPTIMIZATION IN RSM

IPMSM Model	Arc_#0	Arc_#1	Arc_#2	Gap [mm]
Single-layer design		41°~48°	54.2°~59.2°	
Double-layer design	35.4°~41°	46°~52°	54.2°~59.2°	
Novel design_A	35.4°~41°	46°~52°	54.2°~59.2°	
Novel design_B	35.4°~41°	90°~130°		0.35~0.6

*Novel design_B keep outer layer flux-barrier the same as optimal design_A.

The flux-barrier in the double-layer IPM rotor model is optimized by using RSM as an example. Table II lists the experiment ranges of each design variables in RSM analysis, and simulation models are built according to the full factorial combinations of design variables. With the chosen three design variables [Arc_#0, Arc_#1, Arc_#2], fifteen different models are required to be analyzed, as TABLE III lists.

In the RSM optimization analysis, the basic design objectives are determined as: toque ripple at rated operation low than 10[%] and cogging torque amplitude (peak-peak value) less than 3[%] of rated torque 5.5[Nm], nearly 0.16 [Nm], as well the THD of Back-EMF low than 4.0[%]. In addition, the output torque and power constraints are given as:

- Design objectives:

$\mathbf{Y}_{\text{Trip}} \le 10.0[\%], \quad \mathbf{Y}_{\text{CT(p-p)}} \le 0.16[\text{Nm}], \quad \mathbf{Y}_{\text{THD}} \le 4.0[\%]$

- Subject to:

$\mathbf{Y}_{\text{Tave}} \ge 5.5[\text{Nm}], \quad \text{Output power} \ge 2[\text{kW}]$

The responses of design objectives with all design variables are displayed in Fig. 5. It is found the desired minimum points of torque ripple and cogging torque can not be achieved at the same design point. Therefore, the optimum point is selected as possible as close to satisfy all design requirements. With satisfying all design objectives, the optimal double-layer design IPMSM model is built using the corresponding design variables, as each "crossing lines" corresponded in Fig. 5.

TABLE III
DESIGN VARIABLES AND RESPONSES OF RSM SIMULATION

Arc_#0	Arc_#1	Arc_#2	$\mathbf{Y}_{\text{Trip}}$ [%]	$\mathbf{Y}_{\text{CT(P-P)}}$[Nm]	$\mathbf{Y}_{\text{THD}}$[%]
36.5°	47.35°	55.15°	15.86	0.055	3.05
39.8°	47.35°	55.15°	15.23	0.156	4.04
36.5°	50.8°	55.15°	12.57	0.088	3.32
39.8°	50.8°	55.15°	12.50	0.090	3.96
36.5°	47.35°	58.15°	14.60	0.055	3.61
39.8°	47.35°	58.15°	13.51	0.150	4.57
36.5°	50.8°	58.15°	10.54	0.087	4.84
39.8°	50.8°	58.15°	9.56	0.084	5.39
35.4°	49.08°	56.65°	10.75	0.176	4.08
41.0°	49.08°	56.65°	11.07	0.140	4.41
38.15°	46.0°	56.65°	14.41	0.087	5.01
38.15°	52.0°	56.65°	10.41	0.054	4.38
38.15°	49.08°	54.2°	15.83	0.092	3.55
38.15°	49.08°	59.2°	14.23	0.087	5.00
38.15°	49.08°	56.65°	12.89	0.091	4.22

* " " : according to the variables experiment ranges as TABLE I lists.

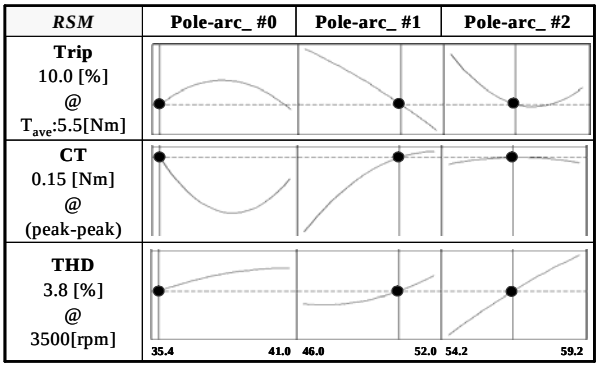

Fig. 5. Response of design objectives based on design variables in RSM

TABLE IV
OPTIMAL VALUES OF FLUX-BARRIER DESIGNS IN IPMSM

IPMSM Model	Arc_#0	Arc_#1	Arc_#2	Gap [mm]
Single-layer design		46.0°	58.0°	
Double-layer design	35.4°	50.4°	56.6°	
Novel design_A	36.0°	52.0°	59.0°	
Novel design_B	35.5°	126.3°		0.5

IV. RESULT AND DISCUSS

The torque ripple and cogging torque are reduced by optimizing the shape of flux-barriers in each IPMSM model, as the process of double-layer IPM model optimization. These optimized IPMSM models are built with their respective "fittest value" of design variables determined by RSM, as TABLE IV lists. And then, the simulation results predicted in RSM are verified by FEA. Also, in this study, the optimized double-layer design IPMSM model is fabricated and tested for confirming the validity of calculated results by FEA.

In final, the torque ripple, cogging torque and Back-EMF characteristics of all the optimized four IPMSM models are analyzed using the test proved FEA method, and compared for examining the effectivity of these various flux-barrier designs on torque pulsation reduction.

A. Test of Double-layer IPMSM

The fabricated double-layer IPMSM is tested, as Fig. 6 illustrates. The torque ripple at rated load operation of base speed 3500[rpm] is tested by inputting current I_a=15.3[Arms] with phase angle β=32.5°. It is found that the tested result 7.8[%] is lower than the corresponding FEA result 10.0[%], as Fig. 7 shows. The error is thought caused by the influence of the reduction gear inertial. In addtion, the cogging torque and Back-EMF characteristics are tested, and the measured results show good agreement with FEA results, as Fig. 8 given. The slightly different may be caused by manufacturing.

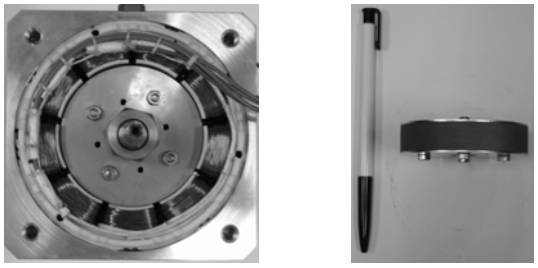

(a) Fabricated optimized double-layer design IPMSM

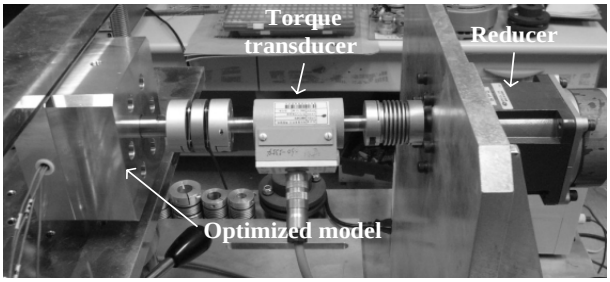

(b) Testing apparatus for torque pulsation measurement

Fig. 6. Output torque test of optimized double-layer IPMSM

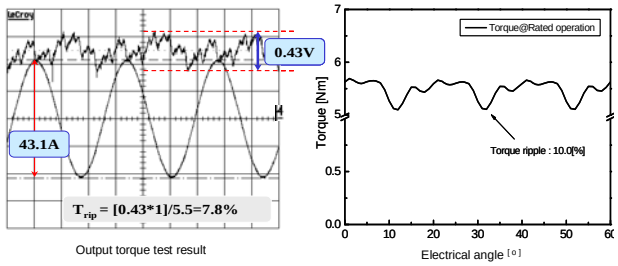

(a) Test result [1V indicates 1Nm] (b) FEA result

Fig. 7. Output torque performance comparison @Rated torque=5.5[Nm].

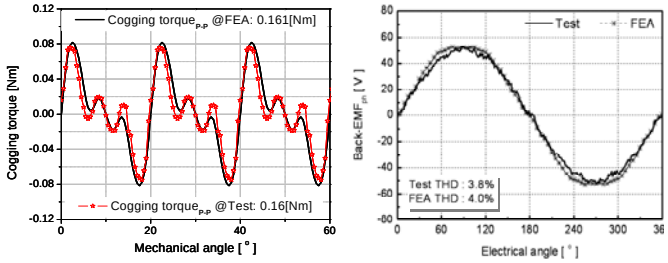

(a) Cogging torque (b) Back-EMF@3500rpm

Fig. 8. Cogging torque and Back-EMF(THD) characteristics comparison

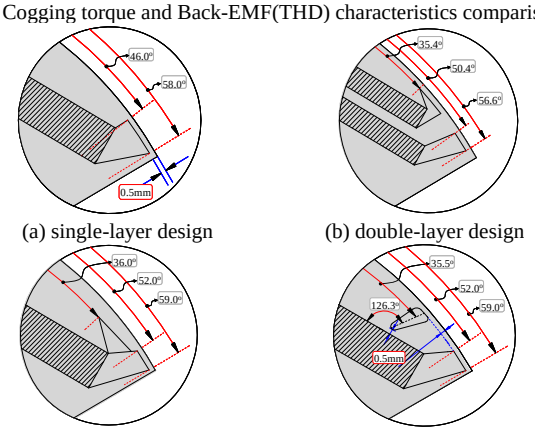

(a) single-layer design (b) double-layer design

(c) novel double-barrier design A (d) novel double-barrier design B

Fig. 9. Optimized flux-barrier designs of IPM rotor model

B. Torque Ripple and Cogging Torque Comparison

Fig. 9 illustrates the geometries of presented four optimized flux-barriers designs of IPM rotor models. The mechanical robustness is considered by margining 0.5[mm] rib thickness between the flux-barrier and rotor surface. From their FEA results of output torque and cogging torque, it is found that the double-layer IPM design and two proposed novel double-barrier IPM designs are effective for reducing the torque ripple and cogging torque. Compare with the optimized single-layer IPM design, the torque ripple of rated torque reduced from 16.5[%] to 10.0[%], 7.0[%] and 5.8[%] separately, and cogging torque relatively decreased 46.7[%], 66.7[%] and 76.7[%] of 0.3[Nm] produced in single-layer IPMSM, as Fig. 11 show. In other words, the amplitudes of cogging torque less than 3.0[%], 1.8[%] and 1.27[%] of rated torque are achieved.

V. CONCLUSION

The reduction of torque ripple and cogging torque by optimizing the various flux-barrier structures in IPMSM were examined in this paper. The novel double-barrier IPM rotor designs were proposed to have beneficial attribute of the flexible flux-barriers design of double-layer IPM design, and

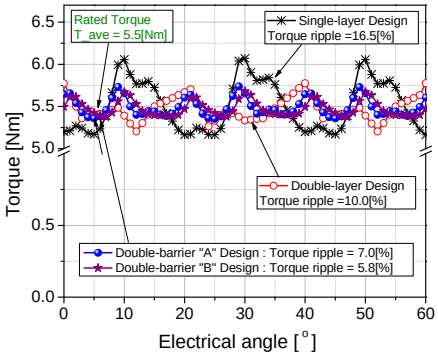

Fig. 10. Torque ripple results comparison by FEA.

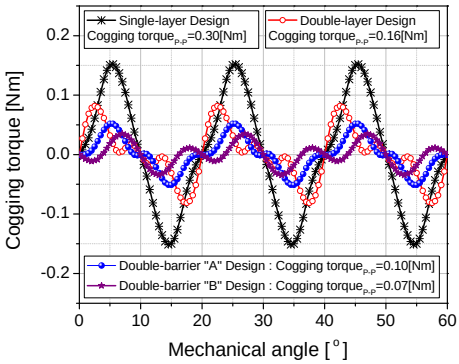

Fig. 11. Cogging torque results comparison by FEA.

the simplicity of single-layer IPM design. The FEA and test results well confirmed the novel double-barrier IPM designs are quite effective on torque pulsation reduction, even better than the popular double-layer IPM design. In conclusion, the novel double-barrier IPM designs have simplicity and low-cost advantages for improving torque performance of IPMSM.

REFERENCES

[1] John M. Miller, "Propulsion systems for hybrid vehicles", The Institution of Electrical Engineers, 2004.

[2] Nicole Bianchi, Thomas M. Jahns, "Design, Analysis, and Control of Interior PM synchronous Machines", *IEEE-IAS Electrical Machines Committee.*

[3] Rakib Islam, Iqbal Husain, Abbas Fardoun, Kevin McLaughlin, "Permanent-Magnet Synchronous Motor Magnet Designs With Skewing for Torque Ripple and Cogging Torque Reduction", *IEEE Transaction on Industry Applications, vol. 45, no. 1, January/February 2009..*

[4] A. Kioumarsi, M. Moallem, B. Fahimi, "Minigation of Torque Ripple in Interior Permanent Magnet Motors by Optimal Shape Design," *IEEE Trans. Magn., vol. 42, Issue 11, Nov. 2006.*

[5] Liang Fang, Jae-woo Jung, Jung-Pyo Hong, Jung-Ho Lee, "Study on High-Efficiency Performance in Interior Permanent-Magnet Synchronous Motor With Double-Layer PM Design," *IEEE Trans. Magn., vol. 44, Issue 11, Part 2, Nov. 2008.*

[6] Ji-Yong Lee, Sang-Ho Lee, Geun-Ho Lee, Jung-Pyo Hong, Jin Hur, "Determination of Parameters Considering Magnetic Nonlinearity in an Interior Permanent Magnet Synchronous Motor," *IEEE Transaction on Magnetics, vol. 402, no. 4, April 2006.*

[7] Sung-Il Kim, Ji-Young Lee, Young-Kyoun Kim, Jung-Pyo Hong, Hur, Y., Yeon-Hwan Jung, "Optimization for reduction of torque ripple in interior permanent magnet motor by using the Taguchi method," *IEEE Trans. Magn., vol. 41, Issue 5, May 2005.*

[8] L. Qinghua, M. A. Jabbar, and M. Khambadkone, "Response surface methodology based design optimization of interior permanent magnet synchronous motors for wide-speed operation," in *Proc. PEMD, vol. 2,* pp. *546-551, March/April 2004.*